Advances in Aircraft and Spacecraft Science, *Vol. 4, No. 2 (2017) 145-167*
DOI: http://dx.doi.org/10.12989/aas.2017.4.2.145

Transonic buffet alleviation on 3D wings: wind tunnel tests and closed-loop control investigations

Arnaud Lepage[*1], Julien Dandois[2a], Arnaud Geeraert[1], Pascal Molton[3], Frédéric Ternoy[4], Jean Bernard Dor[5] and Eric Coustols[5a]

[1]*ONERA, Aeroelasticity and Structural Dynamics Department, Châtillon, 92320, France*
[2]*ONERA, Applied Aerodynamics Department, Meudon, 92190, France*
[3]*ONERA, Fundamental and Experimental Aerodynamics Department, Meudon, 92190, France*
[4]*ONERA, Model Design and Manufacturing Department, Lille, 59000, France*
[5]*ONERA, Aerodynamics and Energetics Modelling Department, Toulouse, 31000, France*

(Received November 13, 2015, Revised September 9, 2016, Accepted September 22, 2016)

Abstract. The presented paper gives an overview of several projects addressing the experimental characterization and control of the buffet phenomenon on 3D turbulent wings in transonic flow conditions. This aerodynamic instability induces strong wall pressure fluctuations and therefore limits flight domain. Consequently, to enlarge the latter but also to provide more flexibility during the design phase, it is interesting to try to delay the buffet onset. This paper summarizes the main investigations leading to the achievement of open and closed-loop buffet control and its experimental demonstration. Several wind tunnel tests campaigns, performed on a 3D half wing/fuselage body, enabled to characterize the buffet aerodynamic instability and to study the efficiency of innovative fluidic control devices designed and manufactured by ONERA. The analysis of the open-loop databases demonstrated the effects on the usual buffet characteristics, especially on the shock location and the separation areas on the wing suction side. Using these results, a closed-loop control methodology based on a quasi-steady approach was defined and several architectures were tested for various parameters such as the input signal, the objective function, the tuning of the feedback gain. All closed-loop methods were implemented on a dSPACE device able to estimate in real time the fluidic actuators command calculated mainly from the unsteady pressure sensors data. The efficiency of delaying the buffet onset or limiting its effects was demonstrated using the quasi-steady closed-loop approach and tested in both research and industrial wind tunnel environments.

Keywords: transonic flow; buffet control; fluidic device; open-loop; closed-loop

1. Introduction

For modern civil aircrafts, the buffet phenomenon remains today a problem of outstanding importance for aircraft designers. In transonic flow, the "buffet" phenomenon refers to a strong shock wave / turbulent boundary layer interaction and massive flow separation located on the upper side of wings at high Mach number and/or high angle of attack. The aircraft structural

∗Corresponding author, Ph.D., E-mail: arnaud.lepage@onera.fr
[a]Ph.D.

http://www.techno-press.org/?journal=aas&subpage=7 ISSN: 2287-528X (Print), 2287-5271 (Online)

response to the aerodynamic excitation is called “buffeting” and may decrease the passenger comfort, increase the structural fatigue and affect the aircraft manoeuvrability. The buffet onset is usually defined by a pilot seat acceleration level and this limit determines the flight envelope in terms of lift coefficient - Mach number boundaries: a 30% margin is required on the cruise lift coefficient.

To get a better knowledge of buffet and to investigate the efficiency of innovative buffet control devices, ONERA took part recently in several projects, national or collaborative research activities (the EU-funded AVERT and Clean Sky projects). At the same time, ONERA launched an internal multi-disciplinary research project (Coustols *et al*. 2009), with the objective to realize the buffet control of 3D turbulent wings in transonic flow conditions and its demonstration during wind tunnel (WT) tests. Therefore, several wind tunnel tests were carried out in the framework of these projects and a large amount of measurements was acquired on two models and in various flow conditions before buffet onset and in buffet conditions.

For buffet control, two innovative fluidic devices/technologies were investigated:

- a “VG-type” (Vortex Generator) actuator, which effect is to add momentum and kinetic energy to the turbulent boundary layer which develops upstream of the shock and the induced separation, in order to suppress or at least delay the appearance of separated unsteady flows, which is at the origin of the buffet phenomenon.
- a “TED-type” (Trailing Edge Device) actuator, which behaves as a thick cambered trailing edge by increasing the rear loading of a wing and then postponing the buffet onset at a higher lift coefficient.

In these works, a special focus was to investigate buffet control thanks to a closed-loop methodology. One major choice at the beginning of these works was to treat the buffet only from an aerodynamic point of view. This led to the use of aerodynamic sensors and actuators, the structural aspects being only considered to verify the efficiency of the control strategies. Therefore fluidic VG and TED devices have been designed, manufactured and tested by ONERA. During the WT tests, the control devices behaviour and their efficiency to decrease the buffet effects or to postpone the buffet onset have been precisely investigated as reported by Molton *et al*. (2013). The analysis of the open-loop databases allowed to identify various strategies for the realization of the active buffet alleviation based on a closed-loop control approach.

This paper will provide a global overview of all experimental activities performed on the buffet and its control through several WT tests. At first, the buffet phenomenon is shortly described and the efficiency of classical or innovative actuators is demonstrated. Then open-loop testing is described in order to characterize the dynamic behaviour of the novel fluidic devices. Finally the control methodology and the closed-loop testing procedures will be described.

2. Experimental roadmap and wind tunnel test campaigns

In order to obtain a reference experimental database, a global roadmap has been decomposed in several wind tunnel tests. The first experimental setup has been tested in the S3Ch research transonic wind tunnel located in the ONERA Meudon Center with the objective to improve the 3D turbulent buffet understanding and to test the efficiency of several actuators. The second phase of the WT tests has been performed in the industrial S2MA wind tunnel of the ONERA Modane-Avrieux Center. This wind tunnel enables to test larger models with specific measurement and test conditions: balance measurements of global forces and moments, continuous variation of the angle

(a) the S3Ch model (a) the S2MA model

Fig. 1 Models in the ONERA WT test sections

of attack (AoA) and adjustment of the WT stagnation pressure (Pi). These characteristics have allowed to extend the parametric analysis of the buffet and to estimate the performances of the various control actuators.

An overview of the models installed in the WT test sections is depicted in Fig. 1. Both wing models represented a "generic" civil transport aircraft composed of a swept wing and a fuselage. A peniche was used to extract the model from the influence of the WT wall boundary layer. The aerodynamic shapes are based on the supercritical ONERA OAT15A airfoil and the sweep angle of the wing is 30°. For the S3Ch test (respectively S2MA), the chord varies from 0.24 m at the root to 0.2 m at the tip over a 0.704 m span (respectively from 0.450m at the root to 0.225 m at the tip over a 1.225 m span). The wing models have been equipped mainly with accelerometers to identify the structural responses and steady and unsteady pressure sensors for the aerodynamic characterization.

These analyses and methodology tests were conducted first in the S3Ch WT then assessed in the S2MA WT and the results presented in this paper mainly refer to the second WT campaign.

3. State of the art of buffet and control with passive/continuous devices

3.1 The buffet phenomenon

The buffet in transonic flow has been experimentally studied for many years, but it is still not completely explained. Data from the state of art indicated that the global mechanisms of the buffet instability for 2D configurations are now well understood (Lee 1990, Jacquin *et al*. 2005, Crouch *et al*. 2009). In transonic flow, the sudden recompression on the upper side of wing generates shock waves which interfere with the boundary layer leading to a potential occurrence of a flow separation. With an increase of Mach number or angle of attack, the flow separation may increase in size and spread from the shock foot to the trailing edge. The shock location oscillates dynamically and modulates the flow separation area. The aerodynamic instability is mainly described by a harmonic behaviour, which frequency and amplitude depend on the shape of the airfoil and on the aerodynamic conditions of the flow. For 3D configurations, the shock wave / boundary layer interactions are also involved in the buffet mechanism but in a wide frequency

band rather than a particular frequency. In fact, the geometrical parameters of the wing are various (sweep angle, aspect ratio, twist law, span-wise effects…) and lead the 3D buffet. Although the global effects of 2D and 3D buffet are identical on the global wings performances (decrease of lift), the physical phenomena involved in the 3D case are more complex and required a specific attention in the view of closed-loop control (Caruana *et al*. 2005).

3.2 Buffet control

There is a huge literature on the control of the shock/boundary layer interaction. The control methods can be gathered into two main categories. In the first category, the objective is to weaken the shock by splitting it to have a bifurcated λ shock structure. Several studies in the last decade have examined passive control devices to bring about the modified shock pattern: a cavity covered with a perforated plate (Bur *et al*. 1998), grooves and stream-wise slots (Smith *et al*. 2003, Holden and Babinsky 2005) underneath the shock foot. These various concepts have led to mitigate success, reduction in wave drag being sometimes negated by viscous penalties (Stanewsky *et al*. 1997). This can be alleviated by using active devices, such as boundary layer suction through a slot, but these devices required auxiliary equipment which offsets any drag reduction benefits (Delery and Bur 2000, Stanewsky *et al*. 2002). A promising method to lowering the total pressure loss through the shock system is the control by a bump. In the beginning, 2D-shape bumps were investigated and led to significant wave drag reductions with moderate viscous penalties, but were found to perform very badly at off-design conditions (Birkemeyer *et al*. 2002). More recent studies were performed with 3D bumps, which have a limited spanwise extent, to enhance the off-design performance (Wong *et al*. 2008, Ogawa *et al*. 2008, Colliss *et al*. 2012). The λ shock structure has been found to propagate between the bumps, giving total pressure decreases across the span. Moreover, streamwise vortices developed along the bump sidewalls have a beneficial effect on the downstream boundary layer behaviour, rendering this passive control device as a promising concept.

The second category aims to energize the boundary layer upstream of the shock making it more resistant to the adverse pressure gradient and consequently less likely to separate downstream of the shock. Mechanical vortex generators (Lin 1991, McCormick 1993, Holden and Babinsky 2007), fluidic vortex generators and synthetic jet fall in this category. Previous studies done at ONERA (Caruana *et al*. 2003) have shown that mechanical VGs are able to delay the buffet onset to higher angles of attack. However, even if they have demonstrated their efficiency for buffet onset delay, mechanical vortex generators have the drawback to increase drag in nominal cruise conditions. This is the reason why fluidic VGs, which can be turned off, are also investigated. Fluidic VGs have mostly been studied to control the shock/boundary layer on a flat plate (Wallis and Stuart 1962, Rao 1988, Pearcey *et al*. 1993, Szwaba *et al*. 2007) and on 2D airfoils (Tilmann 2001, Seifert and Pack 2001, Hassan *et al*. 2007) but there are very few papers on 3D wings.

Regarding the main objectives of the presented paper, very few papers can be found in the literature of an experimental demonstration combining an active buffet alleviation with feedback methodology and an application to 3D configurations. One of the most applied demonstrations through wind tunnel tests has been performed by Moses (1998), Burnham *et al*. (2001). These works describe the development of an advanced buffet load alleviation system that utilizes distributed piezoelectric actuators in conjunction with an active rudder to reduce the structural dynamic response of the vertical tail of an F/A-18 model to buffet loads. Previous works performed at Onera (Caruana *et al*. 2005) have reported a first attempt of buffet control on a 3D

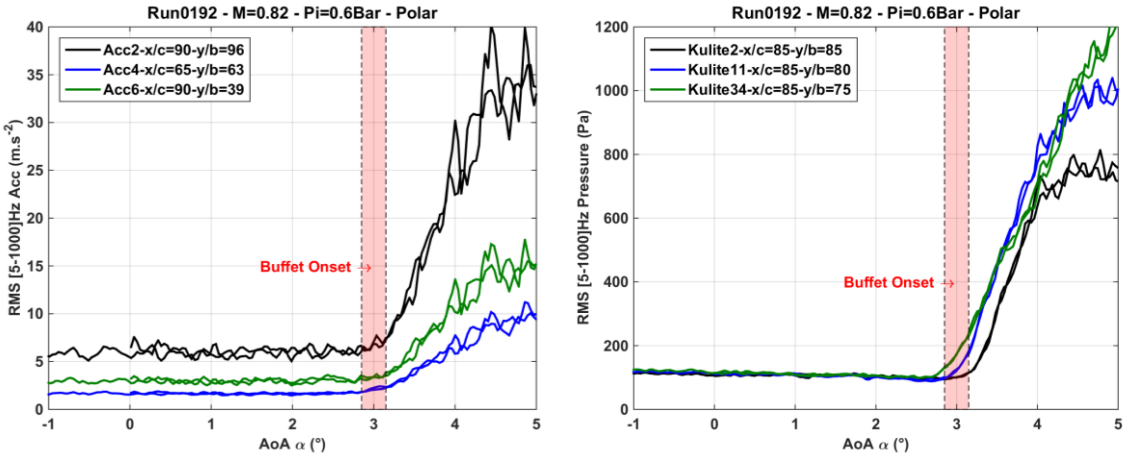

(a) RMS value of acceleration (b) RMS value of pressure

Fig. 2 Illustrations of the different buffet entry criteria for a continuous variation of angle of attack WT @ S2MA-M=0.82, Pi=0.6 Bar, Re=2.83 10^6

wing using a closed-loop approach and mechanical trailing edge deflectors. The buffet control methodology based on the control of the shock location instabilities has demonstrated a great potential but also emphasized the limitations of the device and the complexity to build control laws for buffet alleviation in 3D flow.

3.3 Typical results of the buffet characterization

An important point is to define clearly the buffet onset limit through specific criteria. This will allow to quantify how much a control device is able to suppress the phenomenon or to postpone its onset limit. The buffeting is the dynamic structural response to the aerodynamic buffet excitation. For an aircraft, the buffeting limit during flight tests corresponds to a value of the acceleration measured at the pilot seat. For wind tunnel tests, this criterion is not transposable therefore various criteria have been defined for the buffet / buffeting onset. There are global criteria (based on the kink in the lift curve, the divergence of RMS value of lift or the RMS value of the accelerations) but also local criteria (based on the divergence of the averaged or RMS value of the pressure at the trailing edge).

The Fig. 2 gives an example of criteria on the S2MA model clean configuration, i.e. without control, at Mach number 0.82 and stagnation pressure of Pi=0.6 bar for a continuous variation of angle of attack. On this case, depending on the selected sensor, criteria are in a good agreement with a buffet onset angle of attack equal to 3°±0.1°.

In particular, the pressure data contribute fully to the understanding physical phenomena involved in the buffet and the Fig. 3 presents the steady and unsteady pressure results for the most equipped section (*y/b*=75%) through the visualization of the steady pressure coefficient and RMS value distributions. Up to an angle close to buffet onset, the mean shock position is moving backwards and the "supersonic plateau" level increases. Then, with an increase of the angle of attack, the shock is moving upwards, its oscillation amplitude increases and a separation occurs just upstream of the trailing edge. The distribution of RMS values presented in Fig. 3(b) is

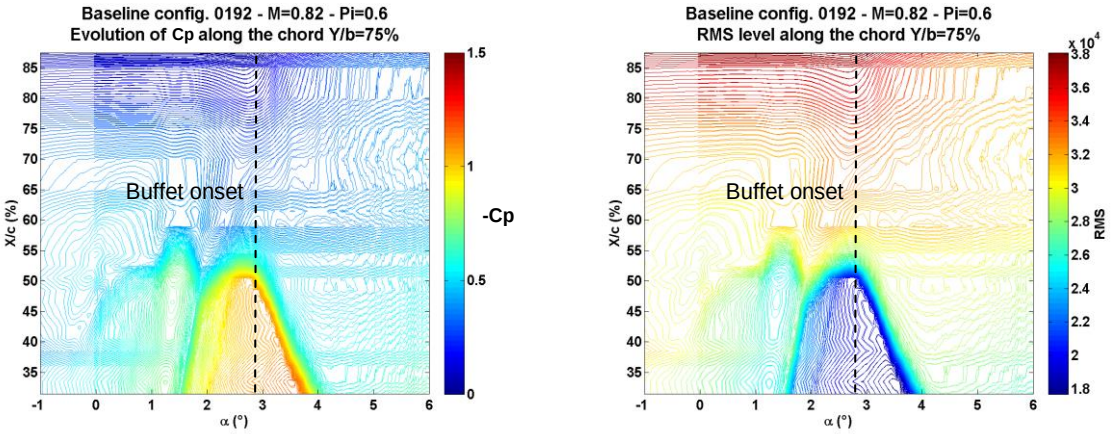

(a) Averaged pressure coefficient (b) RMS pressure value

Fig. 3 Distributions pressure value for a continuous variation of angle of attack WT @ S2MA-M=0.82, Pi=0.6 Bar, Re=2.83 10^6

perfectly consistent with the pressure coefficients distribution. Considering the unsteady pressure transducer located near the trailing edge, the pressure coefficient and the RMS value remain mainly constant for low angle of attack. Then both criteria indicate clearly the appearance of a separated area which intensity increases strongly at very high angle of attack.

The behaviours of the shock location and the flow separation at the trailing edge are typical characteristic of the buffet phenomenon and can be considered as potential inputs to be used in the closed-loop control strategies.

3.4 Spectral analysis of buffet and buffeting regimes

The Buffet in transonic flow is characterised by strongly unsteady phenomena which require spectral analyses to correctly investigate the involved mechanisms. Fig. 4(a) and Fig. 5(a) provide the spectra representation of a wing tip accelerometer and an unsteady pressure sensor (located on the upper side and close to the trailing edge) for various constant values of angle of attack. In addition, time-frequency analyses during a continuous variation of AoA are shown in Fig. 4(b) and Fig. 5(b). These plots provide the Power Spectral Densities estimation of the signals for each segment of the angle of attack, which varied linearly with time.

As previously introduced in this paper and contrary to the 2D Buffet case (Jacquin *et al*. 2005), no well-marked Buffet frequency can be clearly identified in the pressure data. The buffet onset is visible through an amplification of the unsteadiness close to an angle of attack of 3 but no emergence of a specific spectral peak can be noticed. The pressure spectra shown in Fig. 4(a) relate to broadband frequency phenomena. For strong Buffet conditions (i.e., angle of attack greater than 3.5°), the components remain broadband but centred on a "broad frequency bump" close to 200 Hz.

Regarding the structural data in Fig. 5, the frequencies of structural modes can be tracked during the angle of attack variation. According to pressure data analyses, the Buffet onset is not characterised by the appearance of new frequency components. In literature on Buffet, 2D numerical simulations (Raveh and Dowell 2011) demonstrated at Buffet conditions the possibility

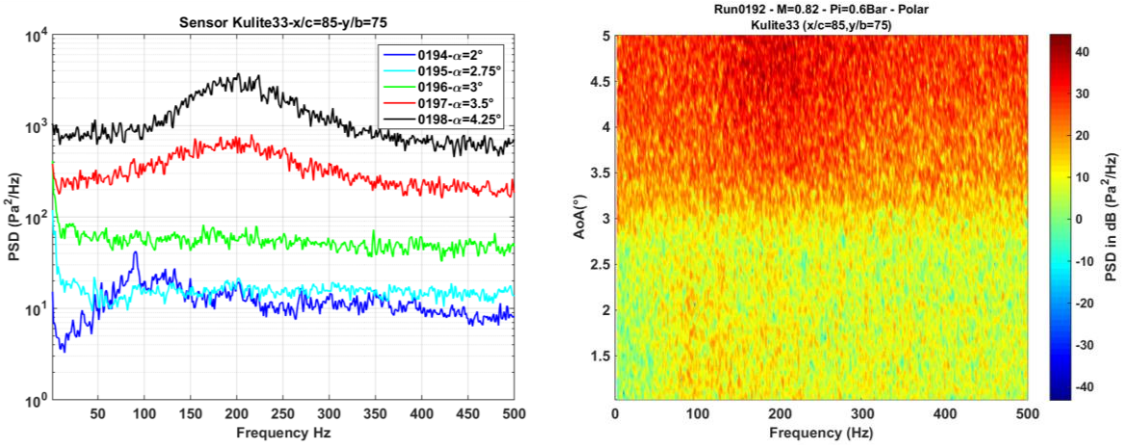

(a) Constant value of angle of attack (b) Continuous variation of angle of attack

Fig. 4 Power spectral density of unsteady pressure signals WT @ S2MA-M=0.82, Pi=0.6 Bar, Re=2.83 10^6

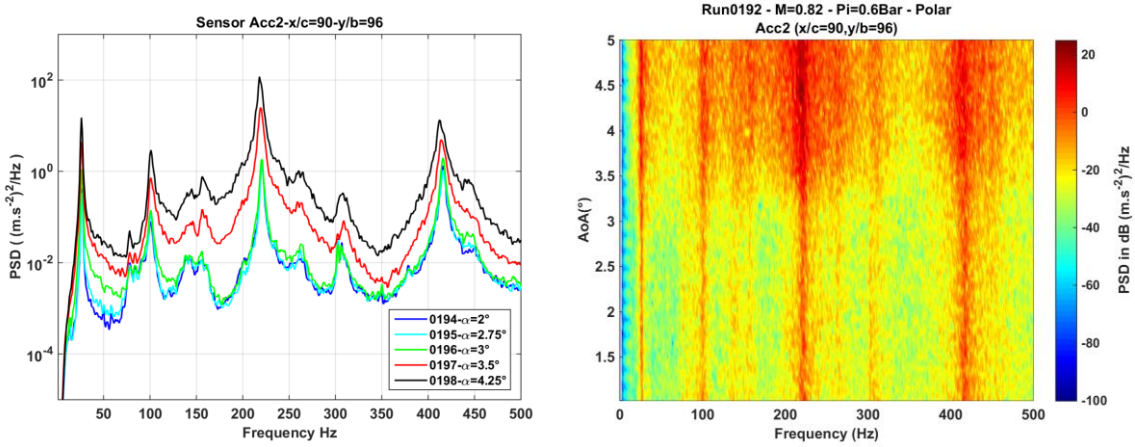

(a) Constant value of angle of attack (b) Continuous variation of angle of attack

Fig. 5 Power spectral density of acceleration signals WT @ S2MA-M=0.82, Pi=0.6 Bar, Re=2.83 10^6

of coupling between aerodynamic and structural mechanisms. Depending on the conditions, a lock-in phenomenon can be observed by synchronising the Buffet frequency with structural motions of the wing. In order to investigate this assumption, a detailed analysis was performed on accelerometers signals. At first, operational modal identification techniques indicated that the modal behaviour of the model was not affected by the buffet onset, showing no significant modification of the modal frequencies and dampings. Then structural responses were analysed on the main frequency peaks to quantify the local dynamic motions of wing sections induced by dynamic motions (bending and torsion motions). Since the model exhibits a high stiffness by design, induced pitch motions appeared to be marginal ($\Delta\alpha$<0.001°) with no direct impact on the Buffet regime. So the structural response levels observed during the WT tests are therefore not linked to a coupling mechanism but simply associated to the forced response of the wing to the aerodynamic perturbation.

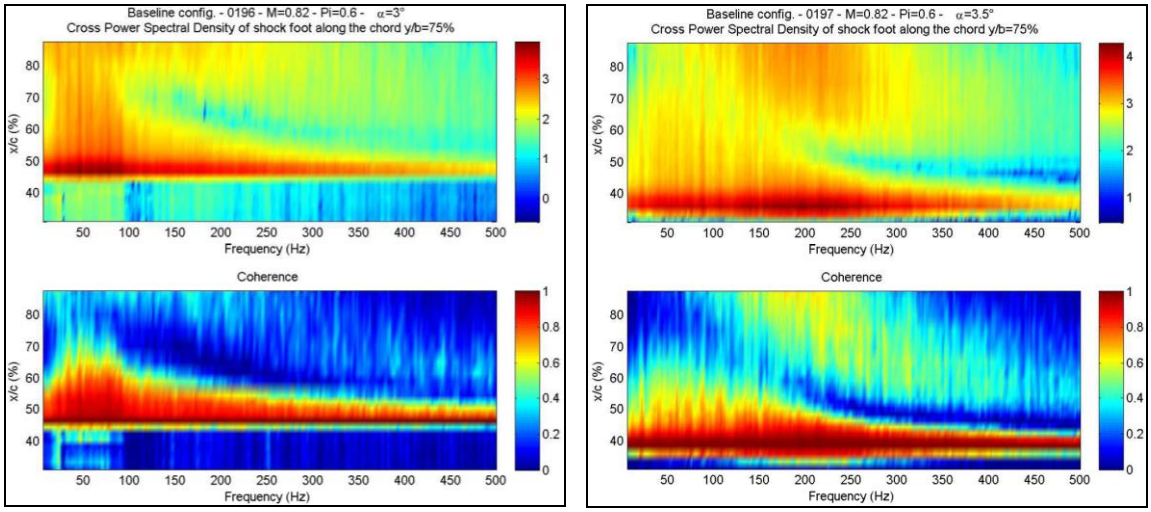

(a) Buffet Onset AoA=3° (b) Strong Buffet AoA=3.5°

Fig. 6 Cross power spectral density and coherence between the unsteady pressures at *y/b*=75% and the unsteady pressure sensor located close to the shock - Baseline configurations WT @ S2MA-M=0.82, Pi=0.6 Bar, Re=2.83 10^6

To investigate more precisely the aerodynamic part, Fig. 6 presents an analysis in the frequency and spatial domains for both buffet onset and strong buffet cases. The data of unsteady pressure sensors distribution at *y/b*=0.75 were used for the calculation of crosspower spectral densities and coherences. For each aerodynamic test point, the reference signal was the nearest unsteady sensor to the steady location of the shock foot. For the buffet onset - Fig. 6(a), the pressure distribution located downstream of the shock is highly correlated to the pressure at the shock foot with low frequency components [0-100] Hz. Nevertheless, the coherence decreases strongly when looking at locations close to the trailing edge. For the strong buffet condition - Fig. 6(b), the observations are similar but for a wider frequency bandwidth [0-200] Hz. Moreover the coherence function indicates that a part of the phenomena at trailing edge (flow separation for *x/c*>0.6) are clearly linked with the ones at shock foot in the range of [150-300] Hz.

These analyses confirm that the 3D Buffet on turbulent wing is characterized by broadband frequency phenomena with spatial and frequency dispersions depending on the considered buffet regime (i.e., before buffet, at buffet onset or for a strong buffet case).

3.5 Buffet control by mechanical vortex generators

For more than 50 years, the aeronautical industry is using mechanical VGs, i.e., located metal tabs angled slightly relative to the airflow, on portions of the upper surface of a wing and placed in a spanwise line. These devices control the airflow over an airfoil by creating a vortex that energize the boundary layer which becomes more resistant to flow separation. This results in an improvement of the aerodynamic characteristics over a wide range of flight conditions (e.g., from low airspeeds to cruise flight, for high load and/or high angles of attack) especially for the buffet phenomenon on 3D turbulent wings in transonic flow conditions.

During the WT Tests in S3Ch and S2MA, the first part of the controlled configuration was

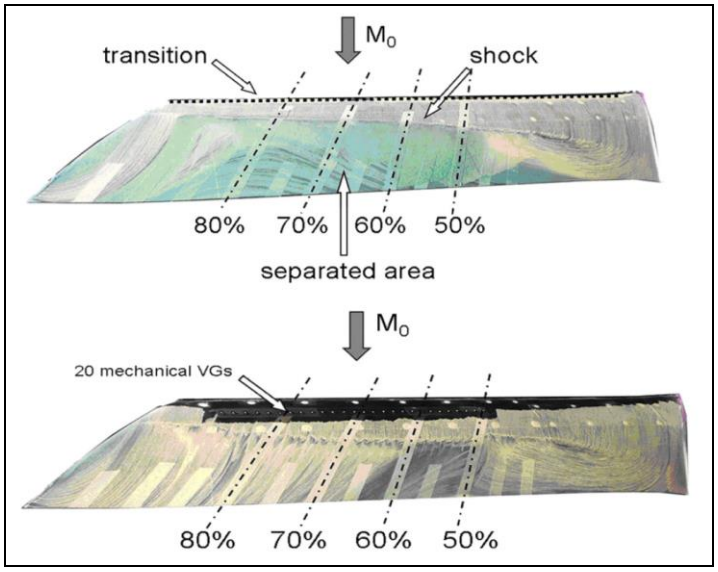

Fig. 7 Oil flow visualization without control (top) and with mechanical VGs (bottom) WT @ S3Ch-M=0.82, Pi=1Bar, AoA=3.5° (Dandois *et al*. 2014)

realized with mechanical VGs. These data defined a reference database with control in order to assess the efficiency of novel fluidic devices. Fig. 7 shows an oil flow visualization of the controlled configurations with mechanical VGs (bottom). By comparing with the baseline without control (top), one can observe that flow separation (in green) has been suppressed over most of the wing span, except between y/b=0.5 and 0.6 where a recirculation zone remains. This is due to the fact that VGs are only located after 50% of the span, which leaves the first half of the wing uncontrolled and prone to separation, like for the baseline.

3.6 Buffet control by continuous blowing fluidic vortex generators

The main objective of using fluidic VGs is to obtain the same efficiency than mechanical VGs with the advantage of a remote control device, i.e., activation/deactivation if necessary. The geometrical parameters of the fluidic VGs were studied numerically to define an optimized architecture as reported by Dandois *et al*. (2013). The fluidic VGs consist in small nozzles with a conical shape and a supersonic exit flow at Mach Number 2. For the S2MA model, a specific model cover was manufactured with 50 fluidic VGs equally spaced between 46% and 89% of the wing span and located at 15% of the chord. A more detailed description on the fluidic actuators in terms of geometry (nozzles diameters, skew and pitch angles …), locations, blowing characteristics can be found in the reference Ternoy *et al*. (2013). The maximum mass flow is 0.5 g/s per hole and the fluidic VGs can operate in continuous or pulsed blowing mode.

The main principle of fluidic VGs is to add momentum and kinetic energy to the turbulent boundary and its action can be quantified by the momentum coefficient $C\mu$ reported by Dandois *et al*. (2013). During the WT test campaigns, several parametric studies have been investigated to analyse the efficiency of fluidic VGs to delay the buffet onset such as mass-flow rate, spacing or spanwise location effects. Main outcomes of the WT tests are described by Dandois *et al*. (2014)

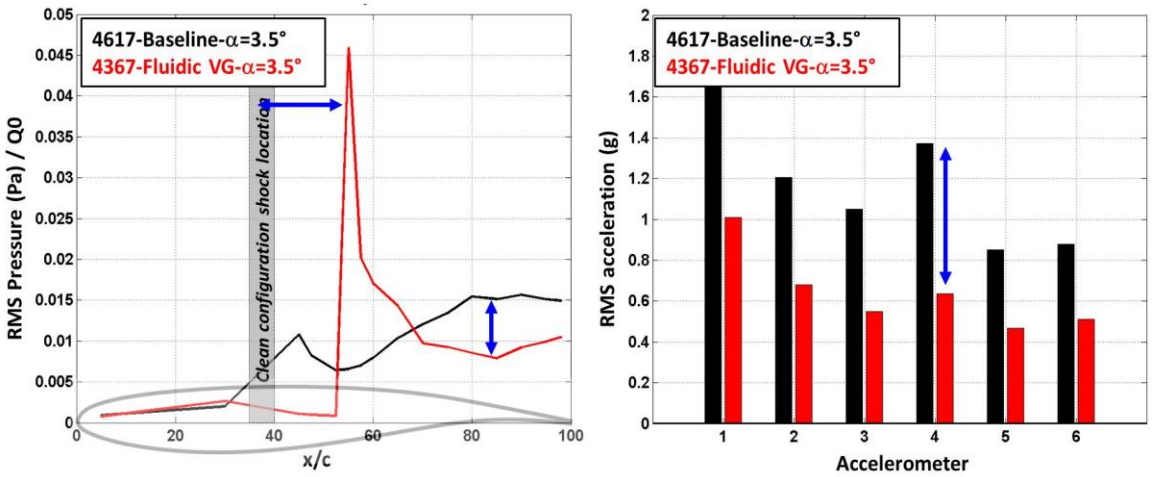

(a) RMS pressure at *y/b*=0.6 (b) accelerations levels

Fig. 8 Comparison for clean and fluidic VGs configurations WT @ S3Ch-M=0.82, Pi=1Bar, AoA=3.5°

and basically illustrated in Fig. 8. The effect of fluidic VGs is comparable to mechanical VGs. As shown in Fig. 8(a), the shock location has been shifted more downstream on the wing. The pressure levels at the trailing edge are lower than for the baseline in all controlled cases demonstrating a flow separation alleviation. This is confirmed by the Fig. 8(a) illustrating that unsteadiness in the separated region has been damped with either passive (mechanical VGs) or active control (fluidic VGs). The effects on the aerodynamic phenomena have a direct influence on the structural model responses. As shown in Fig. 8(b), in all controlled cases (mechanical and fluidic VGs), the vibration levels have been drastically reduced compared to the uncontrolled ones.

3.7 Buffet control by continuous blowing fluidic trailing edge device

The fluidic TED consists in a slot located on the lower side of the model at the trailing-edge with a blowing angle normal to the lower surface. Its design is similar to the one developed for WT tests during the AVERT European project (Dandois *et al*. 2010). The slot is located at *x/c*=0.95 and its width is equal to 0.5 mm. The spanwise length of the slot is 490 mm (between 45% and 85% of wing span). The design and the manufacturing of the plenum that supplies the slot with air were performed at ONERA: 4 transverse sections can be fed separately, the maximum mass flow being equal to 180 g.s-1 (4×45 g.s-1). Fluidic TED can operate in continuous or pulsed blowing mode.

The main principle of fluidic TEDs is to increase the rear loading. As for fluidic VGs, its action can also be quantified by the momentum coefficient Cμ (Dandois *et al*. 2013). During the WT campaigns, several parametric tests have been investigated to analyse the functioning of fluidic TEDs. Main outcomes of the WT tests are reported by Dandois *et al*. (2014). The main conclusion is that fluidic TEDs do not have any (or very few) efficiency on the flow separation and the unsteady phenomena at the trailing edge at the origin of the buffet. This conclusion is pointed out in the next section.

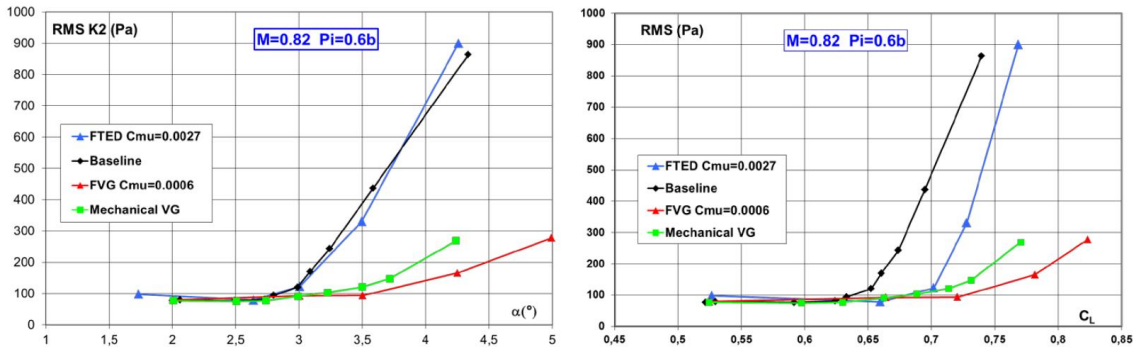

(a) RMS pressure vs the AoA (b) RMS pressure vs the lift coefficient

Fig. 9 Buffet onset for the fluidic and mechanical VGs; Fluidic TED and baseline configurations - Unsteady pressure measurements at (x/c=0.85 y/b=0.75) - WT @ S2MA-M=0.82, Pi=0.6 Bar, Re=2.83 10^6

3.8 Summary of buffet control by passive/continuous devices

The Fig. 9 from Dandois *et al*. (2013) summarizes the main outcomes of the WT tests and the analysis of the buffet onset for all configurations. For the reference case (M=0.82, Pi=0.6bar, Re=2.83 10^6), the RMS fluctuations of an unsteady pressure sensor located on the upper side near the trailing edge are plotted versus the angle of attack and versus the lift coefficient.

For mechanical and fluidic VGs, the strong increase in the pressure fluctuations corresponding to buffet onset is clearly postponed to higher angle-of-attack (Fig. 9(a)) and lift values (Fig. 9(b)). Moreover, the increase in the pressure fluctuations seems to be reduced when buffet becomes stronger and for the considered case, the effects of fluidic VGs are stronger than the mechanical VGs ones.

Concerning the control by fluidic TEDs, the effect of this flow control device does not delay the buffet onset at higher angles of attack (Fig. 9(a)) but only at higher lift values (Fig. 9(b)). Contrary to the VGs devices, the separation downstream of the shock is not suppressed, but the rear wing loading is increased. Consequently the buffet onset is delayed to higher lift coefficient.

4. Performances of active devices for active buffet control

4.1 General considerations in the view of a closed-loop implementation

Previous sections have demonstrated the efficiency of the listed devices to postpone the buffet onset considering a "steady action" of the devices: for the mechanical VGs, the action was purely passive and for the fluidic devices the action referred to a continuous blowing mode.

In order to control Buffet phenomenon using a closed-loop approach, two specific points have to be considered:

- Buffet observability: the ability to have at disposal a sensor or a physical quantity that is representative of the buffet phenomenon. The previous results indicated that the behaviours of the shock location and the flow separation at the trailing edge are typically characteristic of the buffet. The unsteadiness quantity at trailing edge can be directly estimated through an unsteady

pressure sensor. For the shock location, a specific methodology was defined to determine in real time this quantity, based on the estimation of the location of the gradient maximum of an instantaneous pressure distribution (2D assumption - Despré 2001).

• Buffet controllability: the ability of the active fluidic actuators to control the buffet phenomenon through effects on the "buffet sensors". The dynamic functioning of the fluidic VGs and TED are based on ONERA designs using piezoelectric actuators inside the model, supplied with compressed air and driven by electric signals. More details on the dynamic blowing fluidic actuators have been given by Ternoy (2013).

The design specifications and the laboratory tests of the fluidic devices have provided the frequency bandwidth of each actuator. Basically, an electric driving signal commands the mechanical displacement of piezoelectric actuators which pilot the nozzles apertures of the pressurized cavity. A specific feedback loop was tuned in such a way that the resulting flow rate was quasi proportional with the driving signal: frequency or amplitude changes of the command modify similarly the mass flow rate.

The following sections describe the ability of the fluidic devices to act dynamically on the buffet. As the buffet phenomenon is linked to the shock wave / boundary layer interactions, it may appear significant to characterize their dynamic capabilities and especially their respective effects on the shock location and motion.

4.2 Dynamic performances of Fluidic VGs

During the acquisition of open-loops data, a unique command signal drove all fluidic VGs assuming a synchronous functioning (checked during Lab tests). The analysis of the unsteady sensors responses (accelerometers, unsteady pressure sensors, strain gauges) to the known driving signal allows to estimate the behaviour of the whole system and associated phenomena (including the electromechanical behaviour of the actuators, the generation of fluidic jets, the effect of fluidic VG on the external flow, the response of the aeroelastic system).

Typical results are shown in Fig. 10 and refer to a low frequency command imposed to fluidic

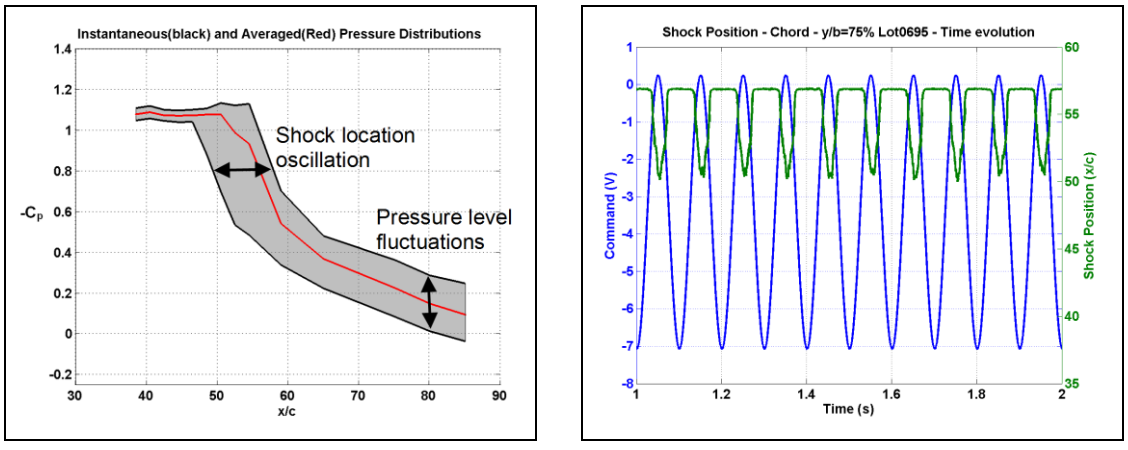

(a) Wall pressure coefficient distributions (b) Shock location and command vs time

Fig. 10 Open loop characterization for a sinusoidal mass flow at f=10Hz : Q(t)=4*(1+sin(2*π*f*t)) with Q(t) in g/s / WT @ S2MA-M=0.82, Pi=0.6 Bar, Re=2.83 10^6 and AoA=3° (buffet onset)

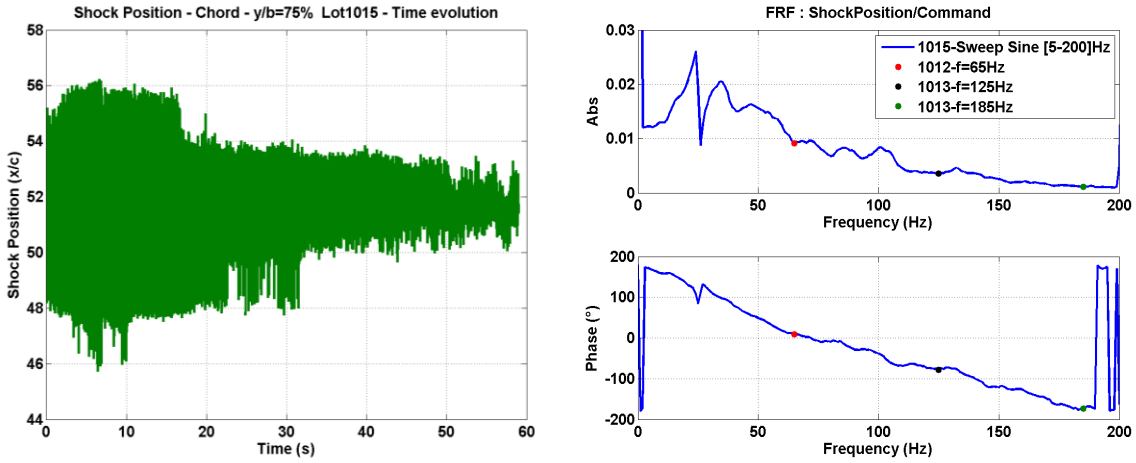

(a) Shock location vs time

(b) Frequency response function: shock location / command signal

Fig. 11 Open loop characterization for a sweep mass flow (f=10→200Hz) : Q(t) = 44*(1+A*sin(2*π*f*t)) with Q(t) in g/s / WT @ S2MA - M=0.82, Pi=0.6 Bar, Re=2.83 10^6 and AoA=3° (buffet onset)

VGs. The analysis of the unsteady pressure sensors located on the upper surface on the chord at y/b=0.75 gives the shock location for each time sample. The envelop of the pressure distribution is described in Fig. 10(a). Using the methodology of instantaneous shock location estimation, the time evolution of the shock location fluctuations is shown in Fig. 10(b). For this test point, the shock oscillates mainly at the frequency of the actuators command with a 7% chordwise amplitude between the uncontrolled location and controlled locations. Complementary, tests were performed for a broad frequency band of the driving signal. The Frequency Response Function (FRF) of the shock location versus the command signal provides a reference curve describing the ability of the dynamic blowing of fluidic VGs to act dynamically the shock location (Dandois *et al*. 2013).

4.3 Dynamic performances of Fluidic TEDs

Similar tests were performed with fluidic TEDs to estimate the dynamic performances of these devices. The Fig. 11 illustrates the actuator effect on the shock location for a sine sweep command. Contrary to the VGs, the TEDs frequency bandwidth was limited to 200 Hz due to mechanical constraints. As shown in Fig. 11(a), the shock oscillates at the driving frequency with a 8% in chord motion at low frequency, the oscillation amplitude decreasing strongly as the frequency increases. The FRF between the shock motion and the actuator command is given in Fig. 11(b). The shape of this curve is similar to the VGs ones: the actuator is clearly able to drive dynamically the shock location over a wide frequency bandwidth (smaller than for the VGs). An event is visible in the vicinity of 25/30 Hz and results from the "forced response" (i.e., strong excitation) of the first structural mode inducing a high level of the structural responses. By principle, the fluidic TEDs generate mainly a normal thrust along the trailing edge which action is very well adapted to excite the first bending mode of the wing for a pulsed functioning close to the associated modal frequency.

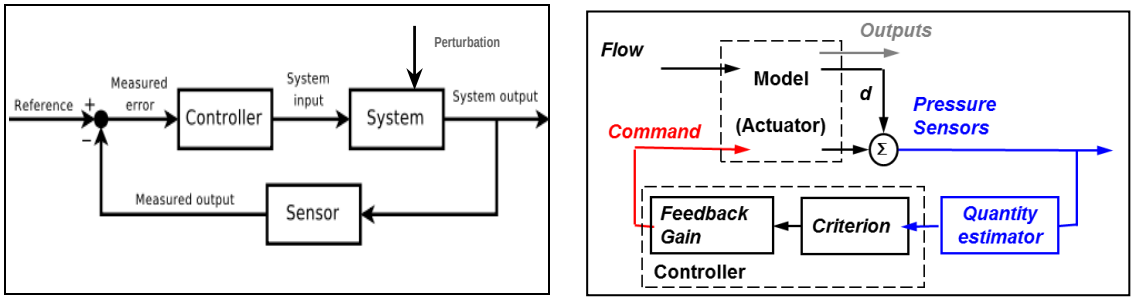

(a) General principle of feedback control (b) Application to buffet control

Fig. 12 Block diagram of the closed-loop control

4.4 Main conclusions in the view of using the closed-loop control theory

The two previous sections have demonstrated the ability of the fluidic actuators to influence the buffet characteristics, especially to move dynamically the shock location. Despite these good open-loop results, various arguments have led to the limitation of using a classical approach of feedback control. Basically, it was not possible to clearly identify a model of the "3D buffet phenomenon" (i.e., the dynamical behaviour of the buffet-flow-model system/plant). The two inputs of the system do not satisfy the classical assumption of exogenous inputs: the control input (i.e. fluidic actuator) is efficient only in presence of the perturbation input (i.e., buffet).

All of these unusual arguments have led to the impossibility or inexpediency to apply an ideal closed-loop approach (i.e., application of the classical feedback control theory). Starting from these conclusions, the strategy was reoriented to realize closed-loop control of the buffet phenomena thanks to a quasi-steady approach aiming at adapting the averaged mass flow rate to the aerodynamic conditions.

5. Active buffet control based on closed-loop approaches

5.1 Principles of the quasi-steady approach

The general principle of a classical feedback loop is presented in Fig. 12(a). The output of the system observed by the sensors is compared to the reference input and the error signal is passed into a compensator and applied to the system. The design problem consists in finding the appropriate compensator such that the closed-loop system is efficient and stable.

The application of a feedback control for buffet phenomena alleviation can be associated to a disturbance rejection strategy. In this case, no reference input is applied to the system, the control architecture aims at minimizing its response to a specific perturbation. For the proposed approach, the quasi steadiness property results from the fact that the system output is passed into an integrator block in order to estimate a specific criterion (RMS value, averaged value) over a "long time" (few seconds) - Fig. 12(b). Several control strategy were investigated depending on the signal/sensor and the objective function used in the closed-loop. For the fluidic VG, two main feedback control architectures were proposed: the first one was based on a trailing edge pressure sensor to act on the flow separation (see 5.3), the second one on a shock location signal "built in

real time" to control the shock wave instability phenomena (Dandois *et al*. 2014). For the fluidic TEDs, referring to the considerations detailed in the section 3.6, a basic closed-loop approach was based on the AoA monitoring and tested during the S2MA campaign.

5.2 Real time control system

All of the methods were implemented on a real time dSPACE device which comprises of several processors and Input/Output boards interlinked for fast internal communication and data exchange. The I/O interface is composed of a maximum of 15 analog inputs and 18 analog outputs. A dedicated computer was used for creating, compiling and implementing Simulink models in the processor boards and a real-time man/machine interface was developed to monitor the signals and change control/command parameters. The schematic control architecture is shown in Fig. 12(b). The control laws were based on unsteady pressure data and used in a SISO configuration (i.e., Single Input Single Output) or MISO (i.e., Multi Input Single Output). All of the fluidic VGs or TEDs were therefore driven synchronously by a unique command signal.

5.3 Closed-loop control with fluidic VGs

5.3.1 Quasi-steady control of the RMS value of an unsteady pressure sensor

The first demonstration was based on the signal of an unsteady pressure sensor located close to trailing edge (x/c=85% and y/b=75%) and a feedback gain manually fixed. The main results are plotted in Fig. 13. Starting from the uncontrolled configuration (fluidic VG command is zero - Fig. 13(a)), the pressure fluctuation levels estimated through the RMS value are very high (Fig. 13(b)). The command of the fluidic VG is determined proportionally to this signal through the feedback loop. As the efficiency of the control modified the signal RMS value, the leading actuation command is adjusted in the same way. After a rise time and settling time, the control command converges to a constant value.

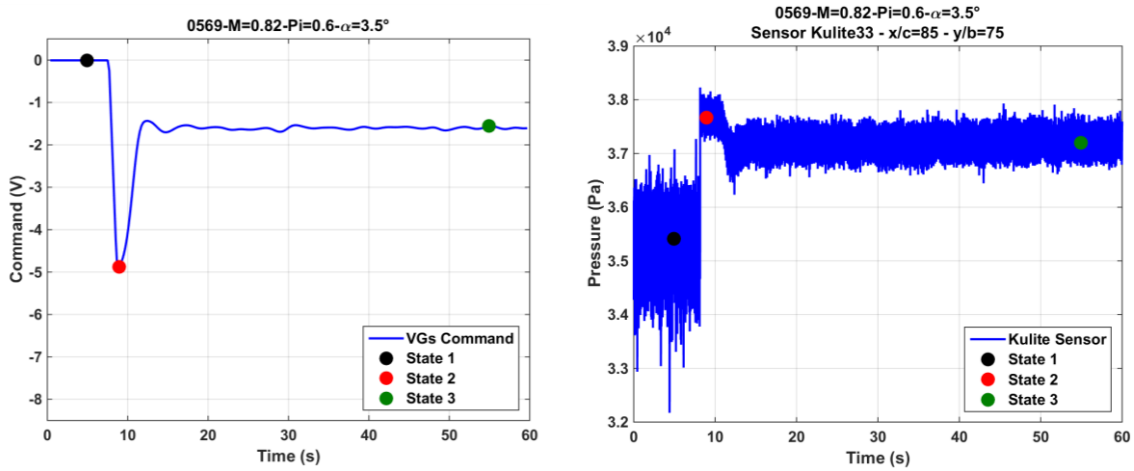

(a) (b)

Fig. 13 Time evolutions of command (a) and pressure signals (b) WT @ S2MA - M=0.82, Pi=0.6 Bar and AoA=3.5°

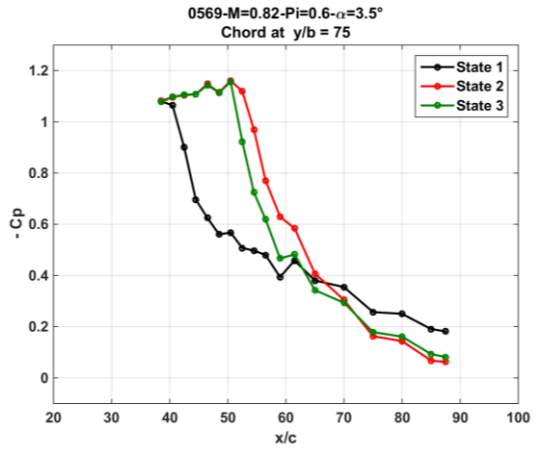

(a) Averaged pressure distribution at *y/b*=75%

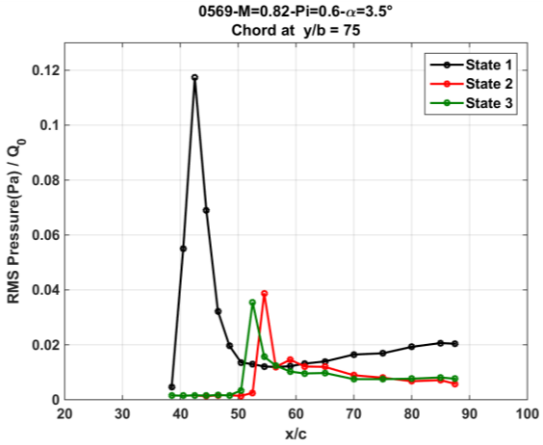

(b) RMS pressure distribution at *y/b*=75%

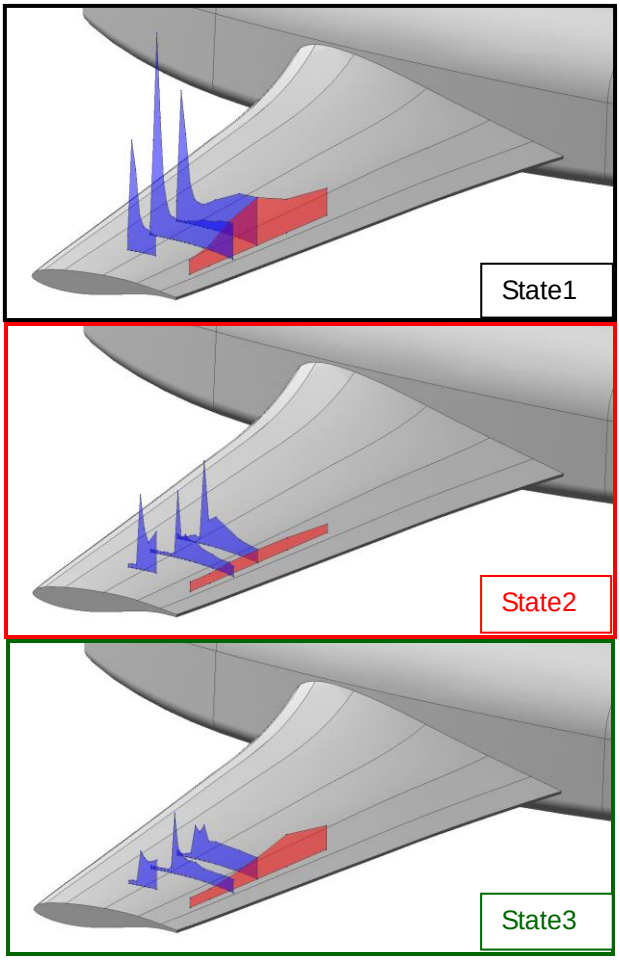

(c) Qualitative overview of control effects - RMS values of pressure (at iso scale) for Chordwise (blue) and Spanwise (red) distributions

Fig. 14 Pressure distributions during a closed-loop control with fluidic VG for 3 temporal snapshots WT @ S2MA-M=0.82, Pi=0.6 Bar and AoA=3.5°

Three temporal snapshots were selected in Fig. 13 and the corresponding wall pressure distributions at *y/b*=75% are presented in Fig. 14. Each curve colour refers to a specific event: black for the uncontrolled state (state 1), red for the maximum flow rate case (state 2) and green for the stabilized state (state 3). After a transient state (in red), the reduction of the RMS value of the unsteady pressure fluctuations are clearly visible at the trailing edge between the black and green curves. This clearly indicates that the flow separation has been strongly reduced or suppressed. At the same time, pressure coefficients (Fig. 14(a)) and RMS (Fig. 14(b)) distributions indicated that the shock is located downstream. Comparing the controlled cases, the figures show a quasi-equivalent efficiency of the control on buffet between the converged state (in green) and the "maximum mass flow rate" state (in red). This point indicates a saturation effect of fluidic VGs as soon as the command (i.e., the mass flow or the momentum coefficient) has reached a threshold.

Fig. 14(c) presents a qualitative overview of the closed-loop control effects on a 3D geometric view of the S2MA model. Each sub-picture refers to a specific temporal snapshot introduced by Fig. 13. The RMS wall pressure distributions are represented in the chordwise (in blue) and spanwise (in red) directions. Comparing the last two pictures with the first one (i.e., no control), the shock location is shifted downstream and the unsteadiness in the separated region is clearly damped over most of the instrumented part of the wing. For the converged state of VGs command (green frame - state 3), a small recirculation zone seems to remain near the mid span area (*y/b*=50%). This is due to the fact that VGs are only located after 50% of the span, which leaves the first half of the wing uncontrolled and prone to separation, like for the baseline. In this case the mass flow rate level (e.g., difference between states 2 and 3) directly impacts the control level of the flow separation in this zone.

An alternative strategy is to use of a "shock location" sensor as control input and built in real time with the monitoring of 10 unsteady sensors. As described in Dandois *et al*. (2014), this approach shows a similar control efficiency by decreasing RMS fluctuations of shock location and shifting downstream its chord location.

5.3.2 Adaptive gain of closed-loop

The previous closed-loop control results were achieved with a manual tuning of the feedback gain. The adjustment of this parameter is a sensitive step which can result in a large change of the performance and the stability of the controlled system. With a small gain value, the actual command might result in an inefficient fluidic VG command or might converge to the desirable output slowly. However, with a large control gain, the actual output might reach the (maximum) saturation value or may never converge (i.e., the controller-plant system oscillates).

In order to avoid the manual tuning of the feedback gain, an adaptive methodology was tested to automatically adjust the proportional gain value using a gradient method. An example is shown in Fig. 15. From the beginning, the first time blocks (i.e., before 30s) are required to adapt the

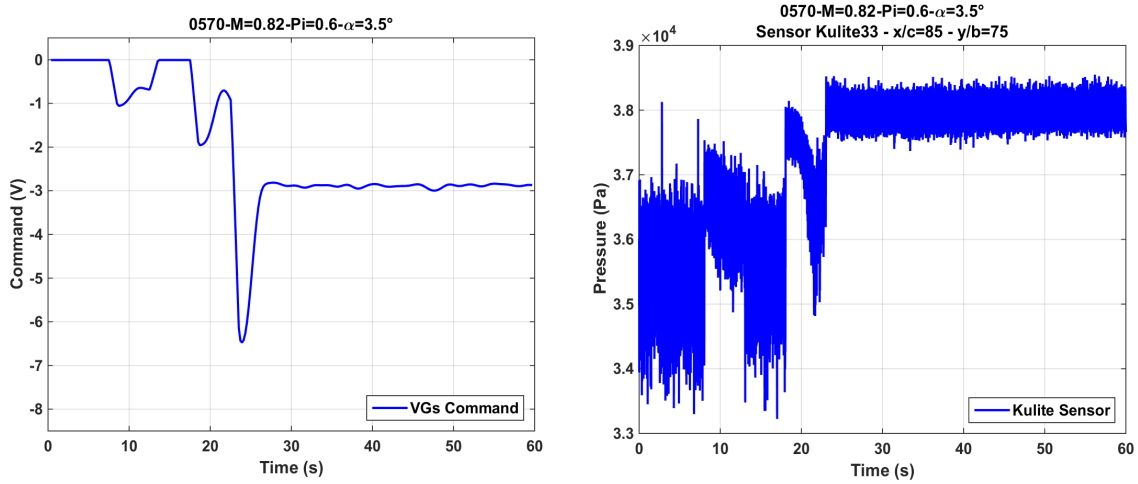

(a) Driving signal of fluidic VGs (b) Unsteady pressure sensor

Fig. 15 Temporal evolutions of input and output signals of the feedback loop WT @ S2MA-M=0.82, Pi=0.6 Bar and AoA=3.5°

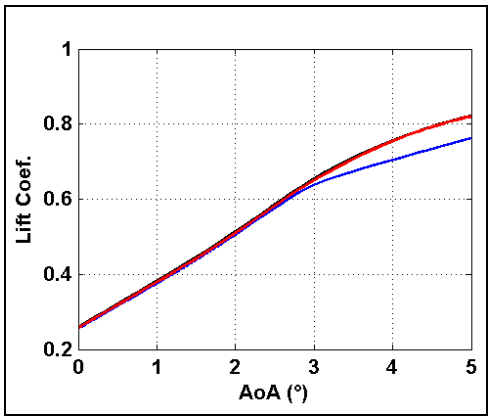

(a) Lift coefficient vs AoA

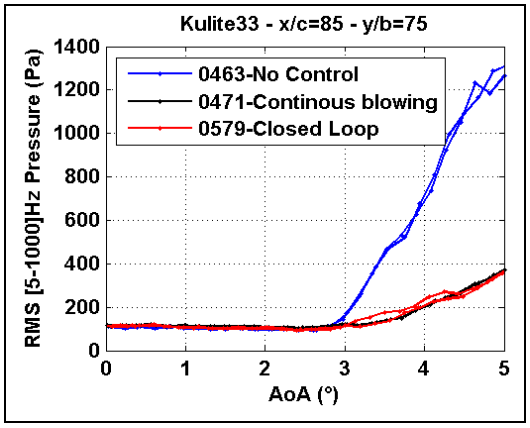

(b) RMS value of pressure vs AoA

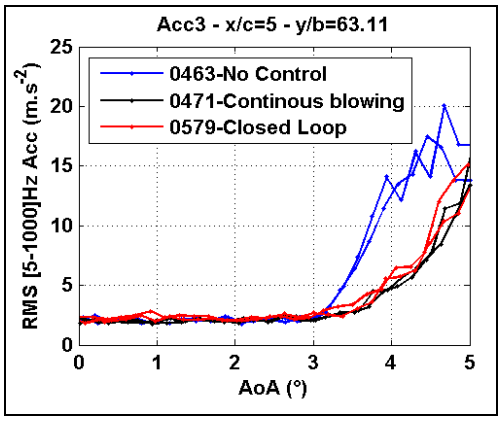

(c) RMS value of acceleration vs AoA

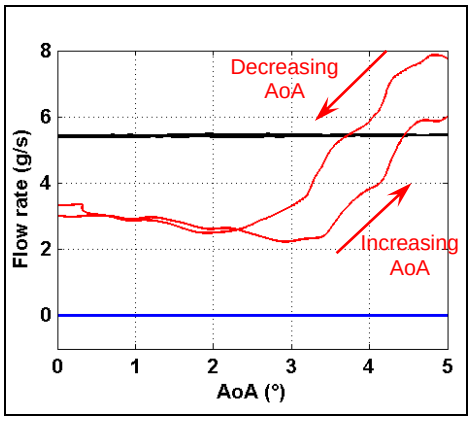

(d) Flow rate of fluidic VGs vs AoA

Fig. 16 Closed-loop Control with fluidic VGs: Evolution of the main parameters during a continuous variation of angle of attack - WT @ S2MA-M=0.82, Pi=0.6 Bar and

output control to a converged value (Fig. 15(a)). Once this state is achieved, the evolution of the pressure sensor located close to the trailing edge indicates the suppression of the flow separation (decrease of pressure unsteadiness levels, increase of the averaged pressure value). Basically, the adaptation procedure does not increase the control efficiency in terms of Buffet alleviation but only provides the possibility to automatize the control process. Nevertheless, it should be noted that as for the manual gain approach, incorrect values of adaptation parameters (e.g., the step size parameter) can lead to an unstable closed-loop.

5.3.3 Basic robustness characterization of a quasi-steady control with Fluidic VGs

As the S2MA wind tunnel enables to achieve tests with continuous variation of the AoA (increasing and decreasing), a simple characterization of the robustness of control strategy was performed. The investigation refers to a quasi-steady control with fluidic VGs, based on an unsteady pressure sensor which signal was fed back through a fixed manual gain. Basically, as the AoA increased, the unsteadiness level rises after the buffet onset requesting a higher level of command and a resulting flow rate.

Regarding the results of the baseline and the continuous blowing configurations, Fig. 16 clearly illustrates the expected effects of the "robust" closed-loop control. The global effect on the lift coefficient in Fig. 16(a) is similar to the continuous control: no effect before the buffet onset and substantial gain after. Looking at a local criterion such as the RMS pressure fluctuation in Fig. 16(b), the conclusions are identical over a wide AoA range. In terms of buffeting, the structural vibration levels are considerably decreased in both cases at the same AoA as shown in Fig. 16(c). Based on these findings in comparison with the open-loop control, the closed-loop approach does not provide any additional impact in terms of alleviation level of Buffet and Buffeting. As the proposed methodology relies on a quasi-steady approach (i.e., slow variations in time), its actual effect tends towards the effect of continuous blowing functioning. However, the use of closed-loop offers the possibility to adapt the fluidic VGs mass flow rate to the aerodynamic conditions. This interesting feature is depicted in Fig. 16(d): the mass flow is proportionally adjusted as the buffet level increases through the variation of AoA. As a result, comparing with the open-loop, this can lead to substantial saving of compressed air requirements which seems to be one of the major constraints for a long-term application on an aircraft. The WT test point presented in Fig. 16(d) is clearly not optimal since the blowing level is not equal to zero before the Buffet onset. Due to time and cost constraints of a test in an industrial WT environment, priority has been given to demonstrating the feasibility and efficiency of a closed-loop control approach. While there remains room for improving the results, the "robustness property" of a closed-loop control demonstrated the possibility to adapt the VGs command to the buffet states.

5.4 Closed-loop control with fluidic TEDs

Contrary to the VGs, the functioning and the efficiency of fluidic TEDs imposed a different approach of a closed-loop control. Indeed, the action of this device does not modify or suppress the buffet characteristics (flow separation, shock motion) but increases significantly the lift. In this case, applying the same closed-loop strategy than for VGs would lead to perform inappropriate comparisons between controlled and uncontrolled configurations. In order to perform a reliable demonstration, an alternative solution would be to have at disposal a parallel closed-loop based on the lift value in order to modify its value (i.e., to remain constant) while in the same time the buffet closed-loop is activated. Unfortunately, the S2MA WT does not have this feature at disposal.

To get around this problem, a basic closed-loop strategy was proposed based on the preliminary knowledge of the buffet vs AoA curve. The open-loop data acquired during an AoA polar were used to define a simplified closed-loop: the fluidic TED flow was driven proportionally to the measured AoA fed back to the real time controller with the definition of "AoA thresholds" for the blowing states (the beginning or the full blowing state). The main objective was to reach with control a targeted lift value outside the buffet. And this lift value refers normally to buffet conditions for the baseline in absence of control (e.g., Cl=0.65). Typical results acquired during an up and down AoA polar are presented in Fig. 17.

During an increasing polar, as soon as the AoA reaches a threshold (AoA=1.75°), the fluidic TED flow rate increases linearly up to a second threshold (AoA=2.25°) and then remains constant. The hysteresis cycle visible in the Fig. 17(d) is linked to the integration time of the data and depends on the polar variation and speed. Basically, the implemented closed-loop strategy indicates a good functioning. The results are consistent with the main conclusions of the section 3.7 devoted to the continuous blowing fluid TED: the actuator command allows to shift the buffet onset at a higher lift coefficient (Fig. 17(a)).

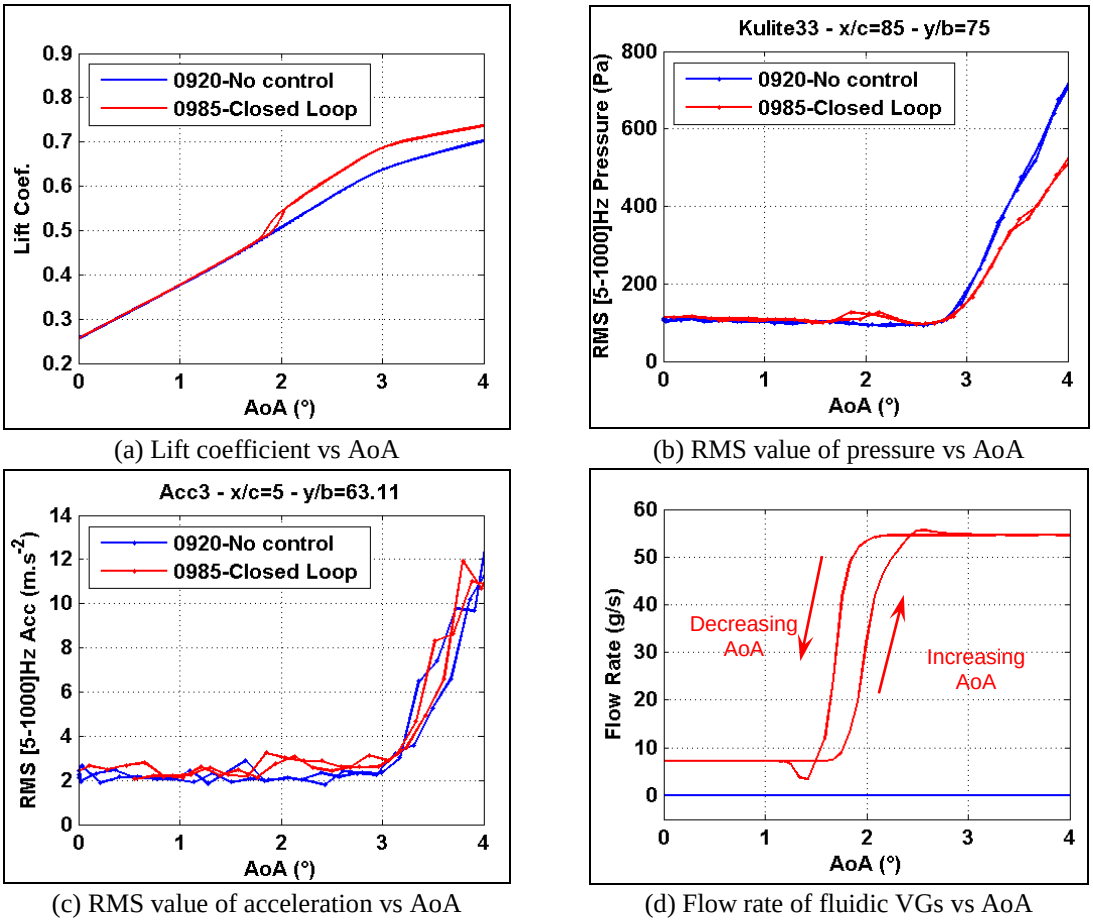

(a) Lift coefficient vs AoA

(b) RMS value of pressure vs AoA

(c) RMS value of acceleration vs AoA

(d) Flow rate of fluidic VGs vs AoA

Fig. 17 Closed-loop Control with fluidic TEDs : Evolution of the main parameters during a continuous variation of angle of attack - WT @ S2MA - M=0.82, Pi=0.6 Bar

Regarding the pressure and structural data (Fig. 17(b) and Fig. 17(c)), the efficiency of the closed-loop did not modify the AoA of the buffet onset. Looking at the acceleration levels, the results appeared quasi-similar without any significant reduction. A small attenuation of the pressure fluctuations levels can be observed on this test point after the buffet onset but the inflection point of the curve still remains at the same angle of attack.

5. Conclusions

The buffet phenomenon remains today a major issue for aircraft since it limits their flight envelope. In this paper, an experimental roadmap based on several wind tunnel tests has been conducted in order to get a better understanding of this phenomenon for 3D turbulent wing in transonic flow. Database analysis was carried out to determine the steady and unsteady mechanisms involved in these flow instabilities. As the transonic buffet on the upper side of a wing is characterized by a shock motion and a massive flow separation, these latter have been analysed

for the definition of active buffet alleviation strategy.

Remote control fluidic devices (Vortex Generators, Trailing Edge Device) were designed and manufactured by ONERA in order to act efficiently on the aerodynamic instability. Their continuous blowing functioning as well as their dynamic behaviour were especially investigated during the WTT campaigns through their effects on the Buffet. The technical developments achieved throughout the duration of each project, were capitalised in terms of actuators design and manufacturing and used in parallel for other applications such as the flow control for high-lift configurations (Brunet *et al*. 2013).

Finally, the demonstration of controlling the buffet using a closed-loop based on a quasi-steady approach was achieved. Different approaches have been developed addressing the adjustment of the actuator mass flow rate thanks to a feedback command based on real time estimation of the shock location or flow separation level. The efficiency of delaying the buffet onset or limiting its effects was successfully demonstrated in both research and industrial wind tunnel environments. In terms of closed-loop control methodology, there is room for improvement especially in the area of the synthesis of a broadband frequency control filter (based on a dynamic model of the plant) for the Buffet alleviation.

The experimental investigations achieved through Wind Tunnel Tests in the S3Ch and S2MA facilities have provided a comprehensive and consistent database. These data are currently used in numerical restitution process for the assessment of high fidelity tools (URANS), especially the ONERA in-house software "elsA" and its capability to reproduce the Buffet phenomenon and the effects of control devices. Furthermore, in the framework of research projects of the Greener Aviation, ONERA is still involved in experimental activities on Transonic Buffet but applied on laminar Buffet (Brion, Dandois *et al*. 2015) which characteristics seem to differ from those in the turbulent case.

Acknowledgments

The research described in this paper was undertaken in the framework of the ONERA's joint research project BUFET'N Co and within two EU-funded projects. The AVERT wind tunnel tests were conducted within the FP6 AVERT European project (Contract N°.: AST5-CT-2006-030914), funded by EC and project partners (Airbus Operations Ltd, Arbus Operations SL, Dassault Aviation, Alenia Aeronautica and Onera). The closed-loop buffet control tests in the S3Ch wind tunnel have received funding from the European Union's Seventh Framework Program (FP7/2007-2013) for the Clean Sky Joint Technology Initiative, under Grant Agreement CSJU-GAM-SFWA-2008-001.

References

Birkemeyer, J., Rosemann, H. and Stanewsky, E. (2000), "Shock control on a swept wing", *Aerospace Sci. Tech.*, **4**, 147-156.

Brion, V., Dandois, D., Abart, J.C. and Paillart, P. (2015), "Experimental analysis of the shock dynamics on a transonic laminar airfoil", *6th EUCASS Conference*, Krakow, Poland, July.

Brunet, V., Dandois, J. and Verbeke, C. (2013), "Flow control for high-lift configurations", *Aerospace Lab.*, **6**(5), 1-12.

Bur, R., Corbel, B. and Délery, J. (1998), "Study of passive control in a transonic shock wave / boundary

layer interaction", *AIAA J.*, **36** (3), 394-400.
Burnham, J.K., Pitt, D.M., White, E.V., Henderson, D.A. and Moses, R.W. (2001), "An advanced buffet load alleviation system", *Proceedings of the 42nd AIAA/ASMBASCE/AHS/ASC Structures, Structural Dynamics, and Materials Conference and Exhibit*, Seattle, WA, April.
Caruana, D., Mignosi, A., Le Pourhiet, A., Corrège, M. and Rodde, A.M. (2005), "Buffet and buffeting control in transonic flows", *Aerospace Sci. Tech.*, **9**, 605-616.
Caruana, D., Mignosi, A., Robitaille, C. and Correge, M. (2003), "Separated flow and buffeting control", *Flow Turbul. Combus.*, **71**, 221-245.
Colliss, S.P., Babinsky, H., Bruce, P.J.K., Nübler, K. and Lutz, T. (2012), "An experimental investigation of three-dimensional shock control bumps applied to transonic airfoils", *AIAA Paper 2012-0043, 50th Aerospace Sciences Meeting*, Nashville, Tennessee, January.
Coustols, E., Brunet, V., Bur, R., Caruana, D. and Sipp, D. (2009), "BUFET'N Co: a joint ONERA research project devoted to buffet control on a transonic 3D wing using a closed-loop approach", *CEAS/KATNET II Conference*, Bremen, May.
Crouch, J.D., Garbaruk, A., Magidov, D. and Travin, A. (2009), "Origin of transonic buffet on aerofoils", *J. Fluid Mech.*, **628**, 357-369.
Dandois, J., Gleyes, C, Dor, J.B., Ternoy, F. and Coustols, E. (2010), "Report on the VZLU wind tunnel test analysis & report on the 3D RANS and URANS computations of mechanical/fluidic VGs and fluidic TEDs", AVERT Deliverables D1.3-3 & D1.3-8, June.
Dandois, J., Lepage, A., Dor, J.B., Molton, P., Ternoy, F., Geeraert, A., Brunet, V. and Coustols, E. (2014), "Open and closed-loop control of transonic buffet on 3D turbulent wing using fluidic devices", *Comptes Rendus Mecanique*, **342** (6-7), 425-436.
Dandois, J., Molton, P., Lepage, A., Geeraert, A., Brunet, V., Dor, J.B. and Coustols, E. (2013), "Buffet characterisation and control for turbulent wings", *Aerospace Lab.*, **6** (1), 1-17.
Délery, J. and Bur, R. (2000), "The physics of shock wave / boundary layer interaction control: last lessons learned", *Proceedings of the ECCOMAS 2000 Congress*, Barcelona, Spain, September.
Despré, C. (2001), "Etude expérimentale et numérique du phénomène de tremblement et de son contrôle en écoulement transsonique bi et tridimensionnel", PhD Thesis, ENSAE, Toulouse, France.
Hassan, A.A., Osborne, B., Schwimley, S. and Billman, G. (2007), "Control of shock-boundary layer interactions (SBLIs) using an oscillatory jet", *AIAA Paper 2007-0476, 45th Aerospace Sciences Meeting and Exhibit*, Reno, NV.
Holden, H.A. and Babinsky, H. (2005), "Separated shock-boundary-layer interaction control using streamwise slots", *J. Aircraft*, **42**(1), 166-171.
Holden, H.A. and Babinsky, H. (2007), "Effect of microvortex generators on separated normal shock / boundary layer interactions", *J. Aircraft*, **44**(1), 170-174.
Jacquin, L., Molton, P., Deck, S., Maury, B. and Soulevant, D. (2005), "An experimental study of shock oscillation over a transonic supercritical profile", *35th AIAA Fluid Dynamic Conference*, Honolulu, June.
Lee, B.H.K. (1990), "Transonic buffet on a supercritical airfoil", *Aeronaut. J.*, **94**, 143-152.
Lin, J.C. (1991), "Exploratory study of vortex-generating devices for turbulent flow separation control", *AIAA Paper 91-0042, 29th Aerospace Sciences Meeting and Exhibit*, Reno, NV, January.
McCormick, D.C. (1993), "Shock-boundary layer interaction with low profile vortex generators and passive cavity", *AIAA J.*, **31**(1), 91-96.
Molton, P., Dandois, J., Lepage, A., Brunet, V. and Bur, R. (2013), "Control of buffet phenomenon on a transonic swept wing", *AIAA J.*, **51** (4), 761-772.
Moses, R.W. (1998), "Active vertical tail buffeting alleviation on an F/A-18 model in a wind tunnel", *Second Joint NASA/FAA/DOD Conference on Aging Aircraft*, Williamsburg.
Ogawa, H., Babinsky, H., Pätzold, M. and Lutz, T. (2008), "Shock-wave / boundary-layer interaction control using three-dimensional bumps for transonic wings", *AIAA J.*, **46**(6), 1442-1452.
Pearcey, H.H., Rao, K. and Sykes, D.M. (1993), "Inclined air-jets used as vortex generators to suppress shock-induced separation", *Paper No. 40 in AGARD CP-534, Fluid Dynamics Panel Symposium on Computational and Experimental Assessment of Jets in Crossflow*, Winchester, UK.

Rao, M.K. (1988), "An experimental investigation of the use of air jet vortex generators to control shock induced boundary layer separation", PhD Dissertation, City University, London.

Raveh, D.E. and Dowell, E.H. (2011), "Frequency lock-in phenomenon for oscillating airfoils in buffeting flows", *J. Fluid Struct.*, **27**, 89-104.

Seifert, A. and Pack, L.G. (2001), "Oscillatory control of shock-induced separation", *J. Aircraft*, **38**(3), 464-472.

Smith, A.N., Holden, H.A., Babinsky, H., Fulker, J.L. and Ashill, P.R. (2003), "Normal shock-wave/turbulent boundary layer interactions in the presence of streamwise slots and grooves", *Aeronaut. J.*, **106**, 493-500

Stanewsky, E., Délery, J., Fulker, J.L. and De Matteis, P. (2002), "Drag reduction by shock and boundary layer control - results of the project EUROSHOCK II", *Synopsis of the Project EUROSHOCK II, Notes on Numerical Fluid Mechanics and Multidisciplinary Design*, Springer Ed., Berlin, Germany, **80**,1-124.

Stanewsky, E., Délery, J., Fulker, J.L. and Geissler, W. (1997), "Drag reduction by passive shock control - results of the project EUROSHOCK", *Synopsis of the Project EUROSHOCK, Notes on Numerical Fluid Mechanics*, 56, Vieweg Ed., Wiesbaden, Germany, **56**, 1-81.

Szwaba, R., Flaszynski, P., Szumbski, J. and Telega, J. (2007), "Shock wave / boundary layer interaction control by air-jet streamwise vortices", *Proceedings of the 8th International Symposium on External and Computational Aerothermodynamics of Internal Flows*, Lyon, France.

Ternoy, F., Dandois, J., David, F. and Pruvost, M. (2013), "Overview of Onera actuators for active flow control", *Aerospace Lab.*, **6** (3), 1-14.

Tilmann, C.P. (2001), "Enhancement of transonic airfoil performance using pulsed jets for separation control", *AIAA Paper 2001-0731, 39th Aerospace Sciences Meeting and Exhibit*, Reno, NV.

Wallis, R.A. and Stuart, C.M. (1962), "On the control of shock-induced boundary-layer separation with discrete air jets", *Aeronautical Research Council C.P. No. 595*.

Wong, W.S., Qin, N., Sellars, N., Holden, H.A. and Babinsky, H. (2008), "A combined experimental and numerical study of flow structures over three-dimensional shock control bumps", *Aerospace Sci. Tech.*, **12**, 436-447.

Acronyms

AoA : Angle of Attack
VG : Vortex Generator
TED : Trailing Edge Device
WT : Wind Tunnel